

**The Characterization of *Drosophila* Shroom**

by

**Lauren M Zasadil**

Submitted to the Graduate Faculty of the  
Department of Biological Sciences in partial fulfillment  
of the requirements for the degree of  
Bachelor of Philosophy

University of Pittsburgh

2010

UNIVERSITY OF PITTSBURGH

Department of Biological Sciences

This thesis was presented

by

Lauren Zasadil

It was defended on

April 22, 2010

and approved by

Dr. Brooke McCartney, Assistant Professor, Carnegie Mellon University

Dr. Beth Stronach, Assistant Professor, University of Pittsburgh

Dr. Vernon Twombly, Lecturer, University of Pittsburgh

Thesis Advisor: Dr. Jeffrey Hildebrand, Associate Professor, University of Pittsburgh

Copyright © by Lauren Zasadil

2010

## The Characterization of *Drosophila* Shroom

Lauren M Zasadil, BPhil, BA

University of Pittsburgh, 2010

Many complex mechanisms regulate cytoskeletal-dependant changes in cell morphology and behavior embryonic and adult life. The actin-binding protein Shroom 3 (Shrm3) appears to interact with Rho kinase (Rok) to direct the assembly of a contractile actomyosin network in neuroepithelial cells, causing apical constriction during neural tube formation. An ortholog of Shrm3 was identified, *Drosophila* Shroom (dShrm), that contains homology to the Shrm3 domain responsible for constriction. When properly targeted, the invertebrate domain also exhibits the ability to cause apical constriction, suggesting that the pathway is conserved in invertebrates. *Drosophila melanogaster* will likely provide a powerful model system to study the localization and function of Shrm during tissue morphogenesis. The project has three goals: to classify the endogenous expression of dShrm, to investigate the effects of over expressing dShrm in various tissues, and to determine a potential interaction between dShrm and dRok. There are two isoforms of dShrm we have primarily studied, dShrmA and dShrmB. Using *in situ* hybridization and immunohistochemistry, we have shown that endogenous dShrm proteins localizes to adherens junctions (dShrmA) and the apical plasma membranes (dShrmB) of cells in the ectoderm, trachea system, and other cell populations during embryogenesis. Over expression of dShrm in the ectoderm, as well as the eye and wing imaginal discs, causes dramatic defects in tissue architecture. Over expression of dShrmA with dRok has shown that there is an interaction between these two proteins. Further work will focus on defining the mechanism by which dShrm functions and which tissues require its activity during embryogenesis.



## TABLE OF CONTENTS

<b>I. INTRODUCTION</b> .....	<b>10</b>
<b>II. AIMS AND HYPOTHESIS</b> .....	<b>17</b>
<b>III. RESULTS</b> .....	<b>18</b>
<b>III A. Endogenous Expression of dShrm</b> .....	<b>19</b>
<b>III A.2 Western blotting and immunostaining to detect dShrm</b> .....	<b>20</b>
<b>III B. Gain-of-function analysis of dShrmA and dShrmB</b> .....	<b>24</b>
<b>III B.2 Phenotypes caused by dShrm over expression</b> .....	<b>28</b>
<b>III B.3 Analysis of dShrmA gain-of-function phenotypes</b> .....	<b>35</b>
<b>III B.4 The role of dRok in dShrm activity</b> .....	<b>39</b>
<b>IV. DISCUSSION</b> .....	<b>41</b>
<b>V. FUTURE EXPERIMENTS</b> .....	<b>44</b>
<b>VI. MATERIALS AND METHODS</b> .....	<b>45</b>
<b>BIBLIOGRAPHY</b> .....	<b>49</b>

## **LIST OF TABLES**

<b>Table 1. Localization and expression effects of Shrm family members .....</b>	<b>41</b>
--	-----------

## LIST OF FIGURES

Figure 1. Schematic of dShrm isoforms.....	12
Figure 2. Schematic of Shrm family members. ....	13
Figure 3. Multiple Sequence Alignment using Clustal X .....	15
Figure 4. dShrm SD2 domain shows conserved function.....	16
Figure 5. RT-PCR gel .....	18
Figure 6. Western Blots.....	19
Figure 7. Endogenous expression of dShrm. ....	21
Figure 8. dShrmA protein is expressed in the ectoderm at the time of gastrulation as morphogenesis is occurring.....	22
Figure 9. dShrm protein is expressed in the invaginating foregut of the embryo .....	22
Figure 10. <i>in situ</i> hybridization of dShrm RNA in a cellular blastoderm .....	23
Figure 11. Localization of ectopic dShrmA and dShrmB in the embryonic ectoderm .....	25
Figure 12. Phenotypes caused by ubiquitous dShrmB over expression.....	27
Figure 13. Expression of ectopic dShrmB alters leading edge cell morphology .....	28
Figure 14. Ectopic dShrmB expression disrupts wing morphogenesis .....	30
Figure 15. Ectopic dShrmB expression alters eye morphogenesis .....	32
Figure 16. Ectopic dShrmA expression causes AJ disruption .....	34

**Figure 17. Ectopic dShrmA expression causes apical constriction ..... 35**

**Figure 18. Ectopic dShrmA causes abnormal cellular morphology..... 37**

**Figure 19. An interaction between dShrm and dRok mediates apical constriction ..... 38**

**Figure 20. Co-expression of a functionally DN-dRok and dShrm inhibits the effects of ectopic dShrm expression by itself ..... 39**

## I. INTRODUCTION

During metazoan development, numerous changes in cell morphology must occur to create tissues of the appropriate fate, size, shape, and position. Epithelial cells, which are present in many tissues in both vertebrates and invertebrates, undergo many changes throughout development (reviewed in [1, 2]). In polarized epithelial cells, the apical and basal surfaces are molecularly distinct, with the apical side facing the lumen [3]. Differential protein expression in these cells effects changes in one part of the cell but leaves the other parts of the cell unaltered. One such change is apical constriction, which shrinks the apical surface area of a cell with relatively few alterations to the rest of the cell [4]. However, there are cases where apical constriction is also associated with increases in either cell height and/or basal width [5]. Apical constriction is achieved by the assembly of contractile actomyosin network within the apical region of the cell which provides the mechanical force to constrict the cell's apical surface [4]. There are two different types of apical contractile networks that can be assembled in polarized epithelia. The first of these is a circumferential actomyosin network that is associated with the apical-most adhesion structure and encircles the entire apical region of the cell [6]. This is the type of network that is seen epithelia comprising many tissues in vertebrates, including the neural plate/tube, retina, intestines, and lung [6, 7]. This is also observed in *Drosophila* tissue such as the lateral ectoderm [8, 9]. The second type is a cortical, mesh-like network that is

associated with the entirety of the apical plasma membrane in polarized cells. This type of network has been best characterized in the ventral furrow of the *Drosophila* embryo [10-12]. It is currently unclear why these two different mechanisms exist, but both have the ability to convert a columnar epithelial cell into a wedge shaped cell. When this type of change in individual cell morphology occurs synchronously in multiple cells in a sheet of cells or a tissue it can cause a change in the overall morphology of the tissue and result in bending or invagination of the tissue [4]. In addition these types of changes in contractility may play key roles in the regulation of overall tissue stiffness or rigidity [13].

Apical constriction is regulated temporally and spatially by numerous signaling and cytoskeletal regulatory proteins, most of which have been characterized in *Drosophila*. These include the secreted factors Fog, Unpaired, Wnt, Hedgehog, and Dpp and cytoplasmic guanine nucleotide exchange factors (Gefs) RhoGef2 and RhoGef64C [8, 14-19]. It should be noted that these pathways and Gefs all serve to activate the small GTPase Rho, which in turn stimulates the catalytic function of the serine/threonine kinase Rock (reviewed in [20]). Rock then regulates the contractile activity of non-muscle myosin II by either directly phosphorylating the myosin regulatory light chain (MRLC) or by phosphorylating and inactivating the myosin light chain phosphatase [21-24]. In the last few years, the Shroom (Shrm) family of proteins has been identified and characterized as an additional pathway that can change cytoskeletal, cellular, and tissue architecture by regulating either the position or activation of actomyosin networks [6, 25]. In vertebrates, Shrm is expressed primarily in polarized epithelial tissues, where it acts to cause constriction of the apical surfaces of cells in a sheet of epithelial tissue, causing an overall morphological change in the tissue [6, 25-29].

Shrm proteins have multiple activities associated with them, which correspond with their identified domains. There are three domains that appear in the family members, although not every domain is found in each member of the Shrm family [30]. The domain closest to the N-terminus is a PDZ domain, which is a structural domain which helps anchor transmembrane proteins to the cytoskeleton and is associated with protein-protein interactions in invertebrates, although it is currently not known what function this domain plays in the activity of vertebrate Shrm proteins. The most central of the domains is an SD1 (Shrm Domain 1) domain, which associates with actin and has been shown to be responsible for localization of the proteins [25, 26]. The C-terminally localized SD2 (Shrm Domain 2) is the last of the conserved motifs and this has been shown to be both necessary and sufficient to cause apical constriction in polarized epithelial cells [6, 26].

In vertebrates, the function of the Shrm family of polypeptides has been an area of research for several years. These studies have resulted in a working model for how the Shrm3 protein causes apical constriction. While this model is specific for Shrm3, we predict that most of the Shrm proteins may function in a similar manner, at least in the regulation of myosin II activity. First, Shrm3 is targeted to stress fibers (composed of actin filaments, crosslinking proteins, and myosin motors), particularly F-actin localized at tight junctions in polarized epithelia. Shrm3 is directly bound to filamentous actin and Rho-kinase, and causes the redistribution of actin as well as contractile activity of non-muscle myosin II [6, 31]. Second, the analysis of the neuroepithelium within Shrm3 null embryos reveals altered distribution of several cytoskeletal proteins, which is caused by the loss of Shrm3 [25]. The interaction between Shrm and Rho-kinase (Rock) causes Rock-mediated phosphorylation of myosin regulatory light chain (MRLC), which controls MyoII activity.

Rok is regulated by auto-inhibitory intramolecular interactions, as well as binding to Rho [23, 32].

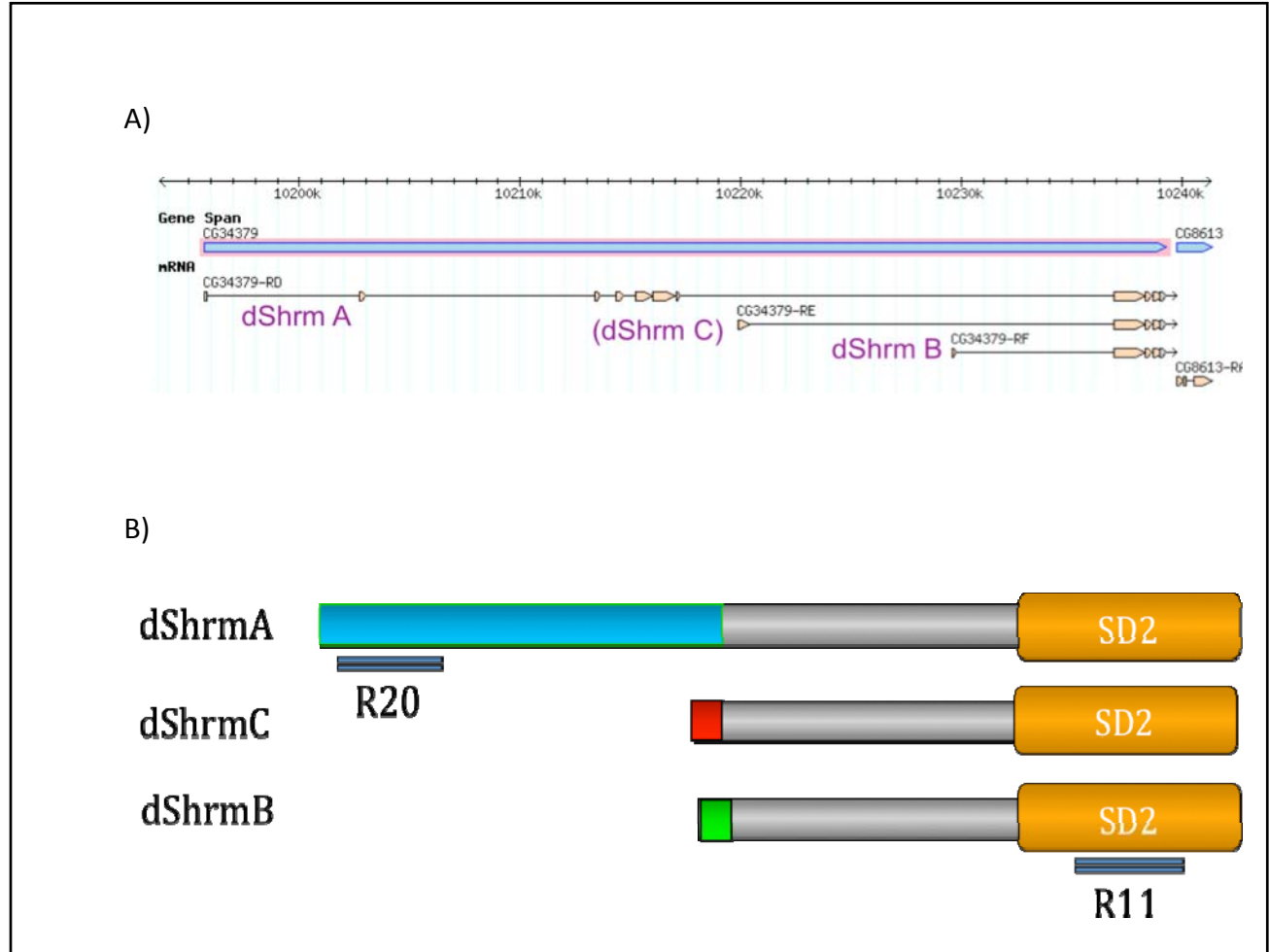


**Figure 1. Schematic of dShrm isoforms. (A), region in the genome that contains dShrm isoforms, and (B) cartoon of dShrm protein products, showing sequence differences (in color) R11 and R20 indicate the region of the proteins detected by the antibodies of these names.**

To date it has been unclear if Shrm functional activities are conserved, particularly in invertebrates, and so a search was done to identify a most divergent family member that would have functional similarities to Shrm. This project started with the initial identification of a gene in *Drosophila* that encodes a protein with limited homology to the Shrm3 SD2 domain [26]. Although *Drosophila* are invertebrates and lack the tissues that

are primarily the focus of vertebrate Shrm work (neural tube and endothelial cells), they do possess analogous tissue types such as the polarized epithelia that undergo many of the complex morphogenic events that are observed in mammals. Many of these are driven by actomyosin networks and involve apical constriction of epithelia. These include but are not limited to ventral furrow formation and invagination of the salivary glands and spiracles.

Based on the annotated *Drosophila* genome, the *Drosophila Shroom* (dShrm) locus is predicted to express at least three distinct protein isoforms, Shroom-PD, Shroom-PF, and Shroom-PG, which have been designated dShrmA, B, and C respectively. The schematic of the locus, the proposed RNA transcripts, and the resultant protein products are depicted in Figure 1. Isoform A is 1576 amino acids long, and isoforms B and C are both 669 amino acids long, varying in their most N-terminal residues. The isoforms B and C both share

near complete sequence identity with the C-terminal part of dShrmA, which contains the SD2 domain and is highly conserved within the Shrm family.

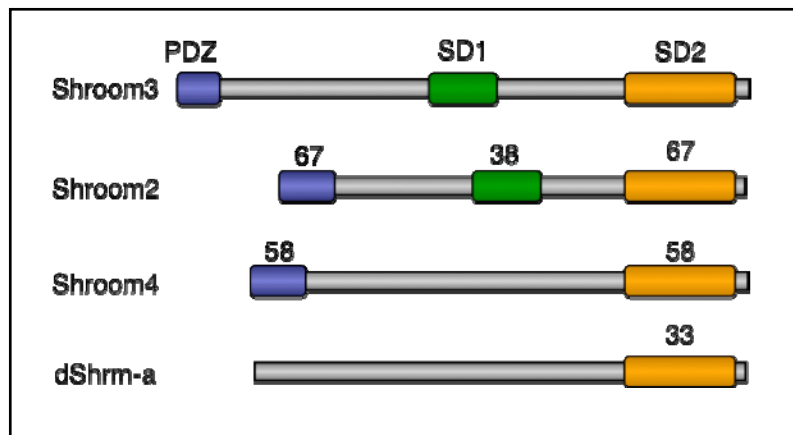


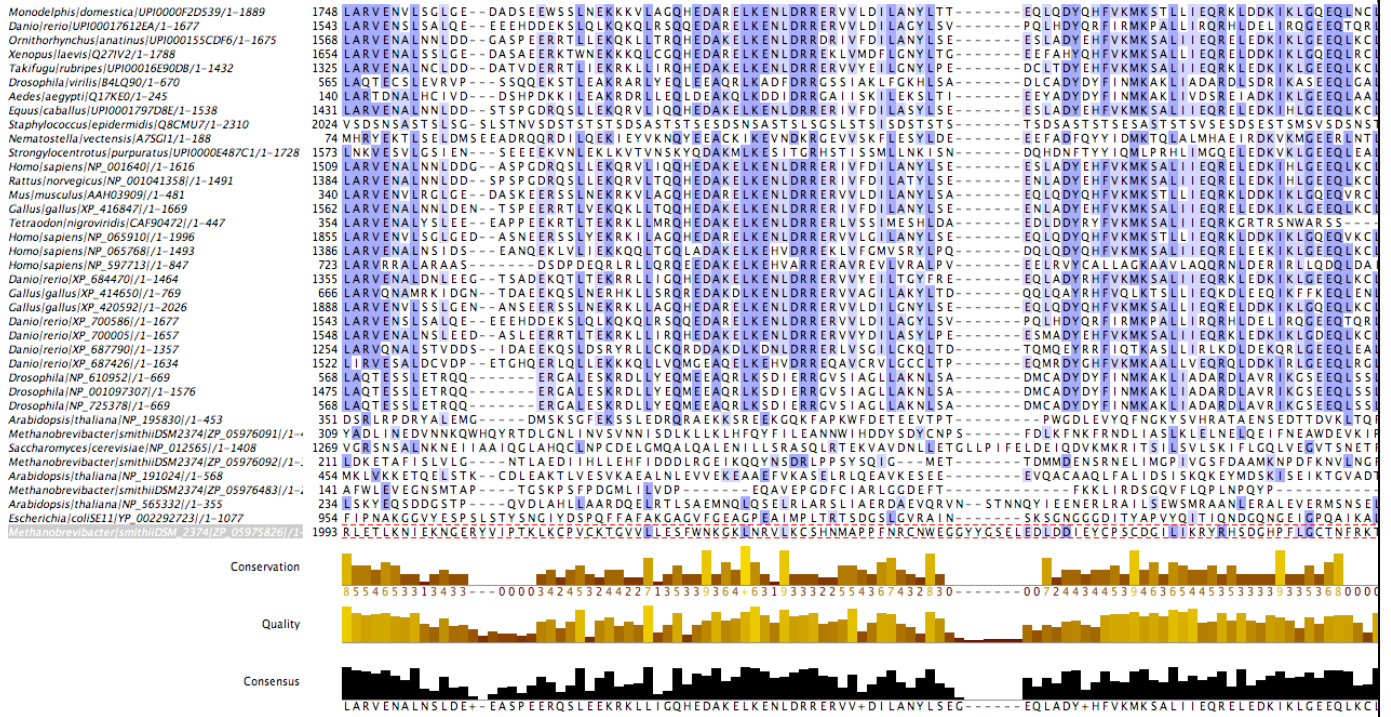
Figure 2. Schematic of Shrm family members. Numbers represent percent conservation to Shrm3

Interestingly, the only portion of the *Drosophila* Shrm that is conserved with vertebrate Shrm proteins is the C-terminal SD2 motif. As can be seen in Figure 2, the dShrm SD2 domain shares 33% conservation with the Shrm3 SD2 domain. This domain is present in all three *Drosophila* isoforms, and is the only region that shows significant conservation among other family

members. Recent experiments suggest that dShrmA does have the ability to bind F-actin using a sequence that has some conservation with the Shrm3 SD1 domain (Hildebrand lab, manuscript in press). Figure 3A displays an alignment showing conservation in the SD2 region of the Shrm family members ranging from vertebrates to plants. Figure 3B shows that the region of the protein closer to the N-terminus lacks significant conservation. There is not only sequence conservation, but also functional conservation of the SD2 domain. When targeted to the tight junctions, SD2 from dShrm also exhibits the ability to cause an apical constriction, suggesting that the Shroom pathway is highly conserved among invertebrates [26]. This is seen in Figure 4, which has the vertebrate SD2 domain replaced by dShrm-SD2. Cells expressing this construct show constriction similar to that caused by Shrm3 [6].

Based on the above information regarding Shrm and *Drosophila* biology, and the long history of *Drosophila* as an outstanding developmental model system for studying the regulation of cellular processes in embryonic and tissue morphogenesis, we believe that *Drosophila melanogaster* could provide a powerful genetic model system to study the function of Shrm proteins. Despite the fact that Shrm proteins have been studied in other vertebrate model systems and tissue culture, there are some significant advantages for undertaking this study of *Drosophila* Shrm. At the time this project was started there was very little evidence that the gene we had identified as the possible Shrm ortholog was indeed the ortholog, and no other invertebrate Shrm proteins had been characterized. In addition, while mice and frog have their advantages for studying the function of Shrm proteins [7, 25, 28, 33], we think that *Drosophila* may provide the best system for doing studies on how Shrm proteins can alter the mechanical properties of cells using live cell

### A) ASD2 region (based on Xenopus)



### B) region without conservation

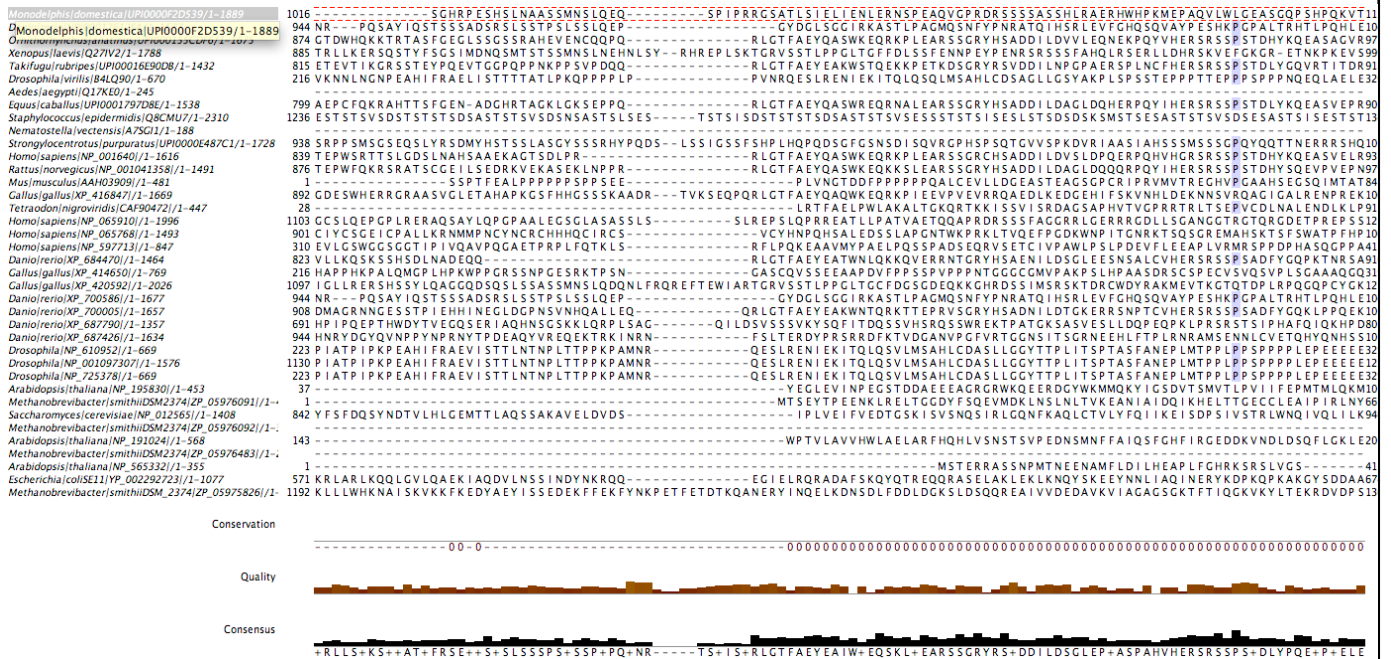
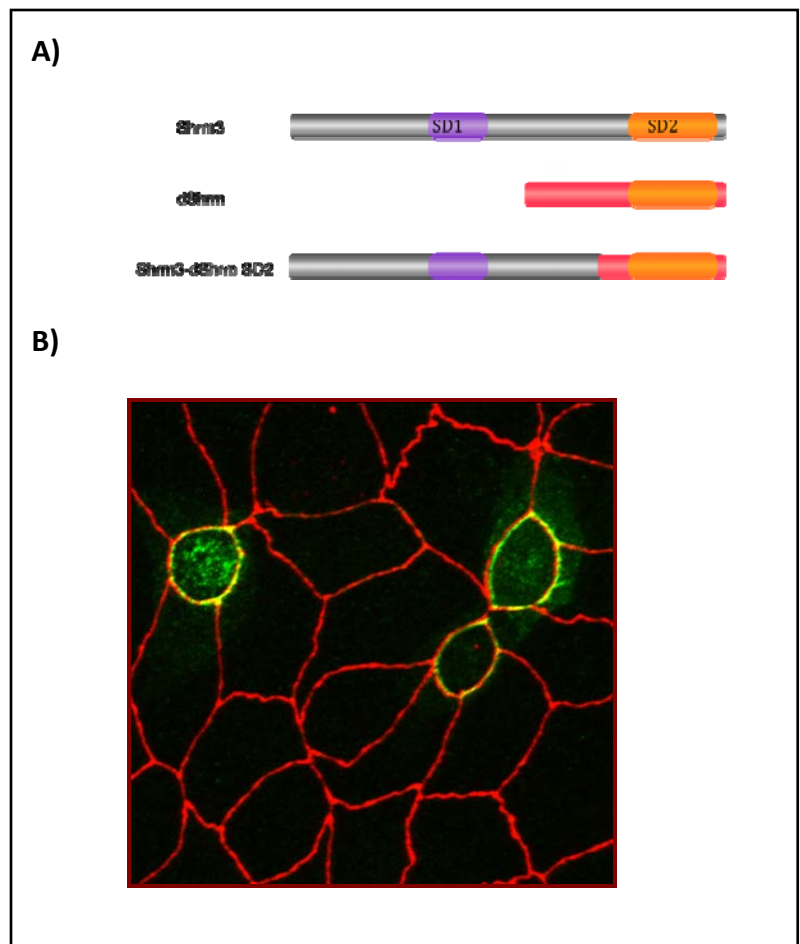


Figure 3. Multiple Sequence Alignment using Clustal X. Conserved residues are shown in blue.

imaging, physical manipulations, and genetic screens to identify other pathways or proteins that might work with Shrm to control cell morphology. In general, *Drosophila* is a useful model system to utilize due to their small size, short generation time, mass numbers, conserved pathways and tissue types with vertebrates, and available molecular genetic tools.



**Figure 4. dShrm SD2 domain shows conserved function. (A) Cartoon representations of Shrm3, dShrmA, and Shrm3-dShrmSD2 construct. (B) MDCK cells transfected with Shrm3-dShrmSD2 construct, stained to detect ZO-1 (red) and Shrm (green)**

## II. AIMS AND HYPOTHESIS

This project has three goals: 1) to classify the endogenous expression of dShrm, 2) to use gain-of-function (over expression) to investigate the activity of dShrm in various tissues during embryonic and larval development, and 3) to determine if dShrm functions with dRok to control cell morphology. Characterizing the endogenous expression data is the first step to understanding if *Drosophila* Shrm has similar function to vertebrate family members *in vivo*, and thus if the function is evolutionarily conserved. The gain-of-function approaches serve as the first attempts to assess if the actual activity of dShrm has been

conserved despite limited sequence conservation. Ectopic expression can also provide valuable information about the subcellular localization of a given protein, and can serve to confirm what is learned from endogenous expression experiments. An interaction between dShrm and dRok would parallel the interaction in vertebrates and further support the evolutionary conservation. We hypothesize that dShrm has similar localization and activity as its vertebrate family members. Furthermore, we predict that *Drosophila* will be an excellent model for studying the Shrm family of proteins. If *Drosophila* provide a useful model for Shrm function, this would allow for faster data collection, increased ability to perform genetic manipulations and genetic screens, and the ability to better utilize live cell imaging and biophysical approaches that are not feasible in other in vivo model system.

### III. RESULTS

At the outset of this project, there was little known about the existence and function of dShrm, and it was not clear that there was a true Shrm ortholog in invertebrates. We identified the putative ortholog based on limited homology to the Shrm3 SD2 domain [26]. At that time, the genome was predicted to encode the isoforms corresponding to what we have termed dShrmB and dShrmC (See Fig 1). The genome was subsequently reannotated to include isoform dShrmA. Our current studies have focused on isoforms dShrmA and dShrmB, as they have the only accessible cDNAs.

### III A. Endogenous Expression of dShrm

The first stage in understanding the *in vivo* function of dShrm proteins is to catalogue when and where these proteins are expressed in the embryo, as well as where the protein is localized within these cells. To do this, we utilized RNA *in situ* hybridization, reverse transcriptase (RT) PCR, western blotting, and immunostaining of embryos and larvae. We used these approaches due to limitations of our antibodies. Specifically, we cannot distinguish between dShrmB and dShrmC, and we can only predict dShrmB/C localization based on

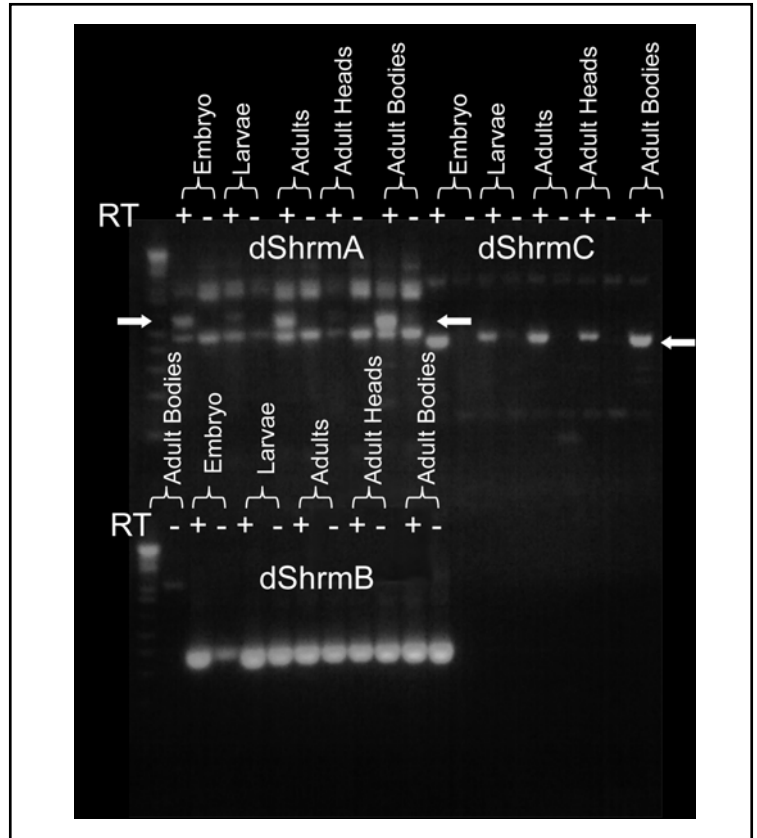


**Figure 5. RT-PCR gel.** Agarose gel from RT-PCR, arrows indicate DNA products of expected size. +/- above lanes indicates the presence or absence of reverse transcriptase

differences in immunostaining between antibodies that recognize only dShrmA,

or all three isoforms. To determine when each isoform was expressed, RT-PCR was performed to generate cDNA from mRNA extracted from embryos, larvae, adults, adult heads, and adult bodies. The results of this gel show that each isoform is present in embryos, larvae, and adults (full, heads, and bodies). Primers were designed to specifically amplify the unique 5' regions of each putative dShrm mRNA. In Figure 5, arrows indicate the location of bands that indicate the positive detection of each isoform. With the primers

that are supposed to be specific to dShrmA, the expected band is in all of the reactions that contained reverse transcriptase (+RT). In addition to the band of the predicted size, we also detect what we predict are non-specific DNA species that were amplified in the PCR reactions. The dShrmC reactions produced cDNA of the expected size in all reactions containing RT and not in any reaction that did not contain RT (-RT). The dShrmB reactions appear to have contamination in them which resulted in a band in every lane. Based on these results, it appears that all three isoforms may be expressed in *Drosophila*.

### III A.2 Western blotting and immunostaining to detect dShrm

In order to more definitively determine where the dShrm protein is expressed and localized, we generated antibodies to the dShrm proteins. Antibodies were generated in rats to the C-terminal conserved domain of the three proteins (R11, Figure 1). To test these antibodies, we isolated protein extracts from either wildtype *w<sup>1118</sup>* embryos or from *w<sup>1118</sup>* embryos over expressing dShrmB. In wildtype embryo

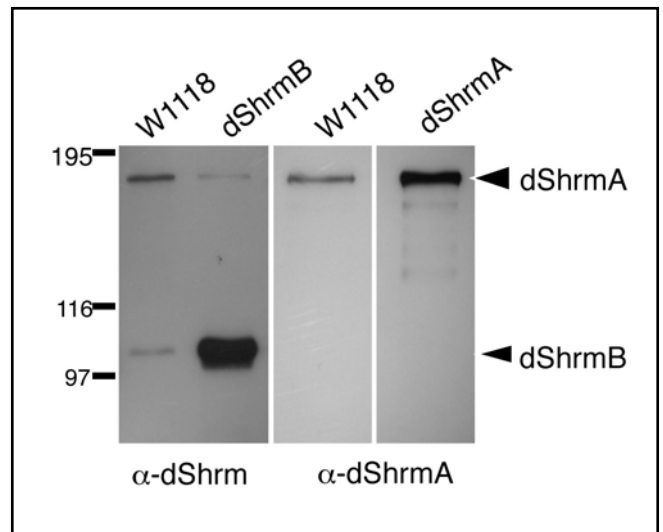


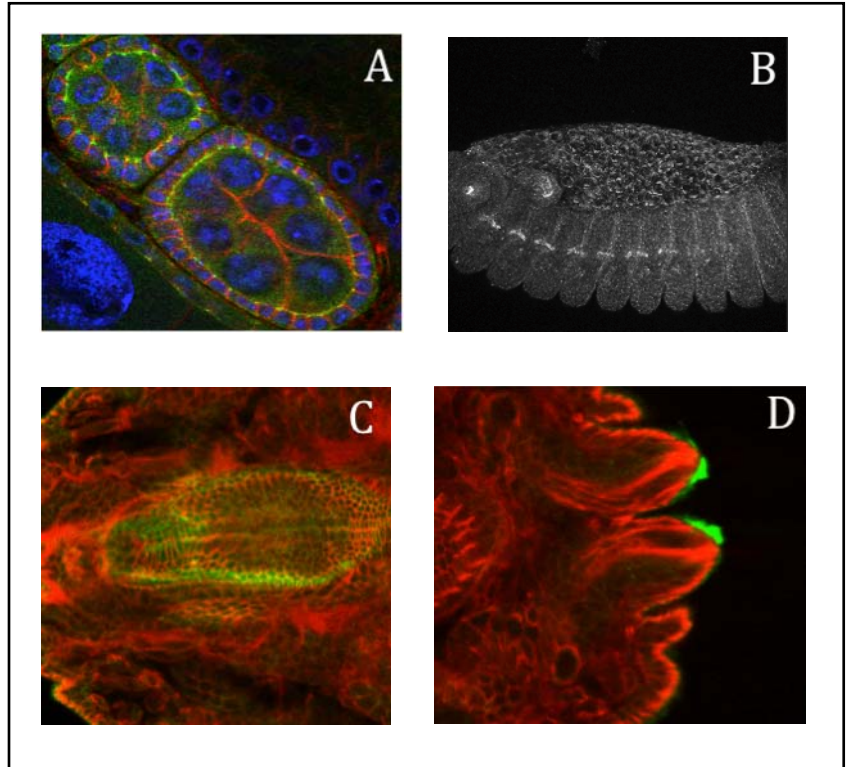
**Figure 6. Western Blots.** Western blots from acrylamide gels probed to detect dShrm with antibodies indicated along the bottom. dShrmA and dShrmB samples were from embryos ubiquitously over expressing the protein, embryos used were up to stage 14.

lysates, we detect two proteins, of 180 kD and 100 kD. We predicted that the lower band corresponds to dShrmB or dShrmC, as it runs at the same molecular mass as the ectopically expressed dShrmB. The upper band is likely dShrmA. This prediction is verified by

western blot analysis using antibodies that are specific to dShrmA (R20, Figure 1). The antibodies specific to the unique region of dShrmA detected only a protein of 180 kD. However, the antibodies generated against the conserved region (R11) recognizes all isoforms, which appears as detection of a 100 kD protein as well as a 180 kD product (presumably dShrmB/C, and dShrmA, respectively). Western blotting of lysates from *w<sup>1118</sup>* or *w<sup>1118</sup>* embryos over expressing dShrmA identifies a single band of about 180 kD. These data show that *in vivo*, dShrmA is the most abundant isoform expressed, but that either dShrmB and/or dShrmC is also expressed at lower levels.

Due to previous work showing that vertebrate Shrm proteins are expressed in various epithelial populations undergoing morphogenesis, we wanted to determine where and when dShrm proteins are expressed, and where the proteins are localized in the embryo. For many of these experiments, embryos were stained with R11, as it gives the best staining results. However, most of the staining was faithfully recapitulated using antibodies specific to dShrmA. Staining with the antibodies generated to all dShrm isoforms was performed on all stages of embryos to detect where dShrm proteins are expressed during embryogenesis and morphogenesis of discs. Wild-type *w<sup>1118</sup>* embryos showed no immunofluorescent detection prior to gastrulation. After the start of gastrulation, however, dShrm proteins become detectable. Past stage 7, which marks the start of gastrulation, dShrm is detectable at cell-cell junctions in the epithelia of embryos. By stage 10, dShrmA can be seen localized to tri-cellular junctions. This was further clarified by costaining with Armadillo, which localizes to adherens junctions (AJs). We predict that this represents dShrmA, as it can be detected with both R11 and R20.

Various staining patterns detected with dShrm antibodies are seen in Figure 7. In Fig.7A, dShrm is seen localized to the adherens junction of the follicular epithelium of the adult ovary. There is also endogenous expression of dShrm in the foregut (Fig. 7C) and posterior spiracles (Fig. 7D). In Fig. 7B, dShrmB is



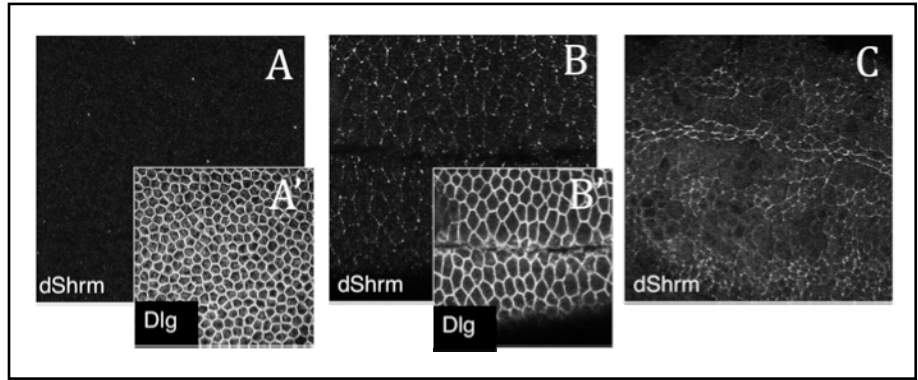
seen localized to the tracheal pits along the side of the embryo. Endogenous detection in the embryonic ectoderm using R20

**Figure 7. Endogenous expression of dShrm. (A), localization of dShrmA/B/C (green) in the adult ovary (red = dlg, blue = TOPRO). (B) dShrmA/B/C detection shows localization in tracheal system as well as throughout the ectoderm. (C), stage 16 embryo showing immunofluorescent detection of dShrmA/B/C (green) in the foregut and (D), posterior spiracles (red = dlg). All images of embryos are oriented with the anterior to the left and posterior to the right.**

shows that dShrmA is undetectable in early embryos (Fig. 8A). At the time of ventral furrow formation, dShrmA becomes detectable (Fig 8B). Later in embryonic development, at the time of germband retraction, dShrmA can be seen localized to the adherens junctions, particularly in the ventral furrow (Fig 8C).

In vertebrates, Shroom proteins are expressed in tissues as they undergo morphological rearrangements such as bending and invagination. This pattern is seen in *Drosophila* as well, as is demonstrated in Figure 9. As foregut invagination occurs, dShrm protein is detected in the constricted cells (A-C), and a lateral view of the cells shows

localization to the adherens junctions (D-F). In summary of this section, it appears that



dShrmA is expressed primarily in populations

**Figure 8. dShrmA protein is expressed in the ectoderm at the time of gastrulation as morphogenesis is occurring. W1118 embryos viewed ventrally side at various developmental stages immunostained to detect dShrmA (large boxes) and Dlg (insets)**

of polarized epithelia beginning at or shortly after gastrulation. There is higher levels of dShrmA observed in the invaginating fore- and hindgut, suggesting this protein could be involved in the morphogenesis of these tissues. In addition, we predict that either dShrmB and/or dShrmC is expressed in epithelial cells that comprise tubes of the tracheal system,

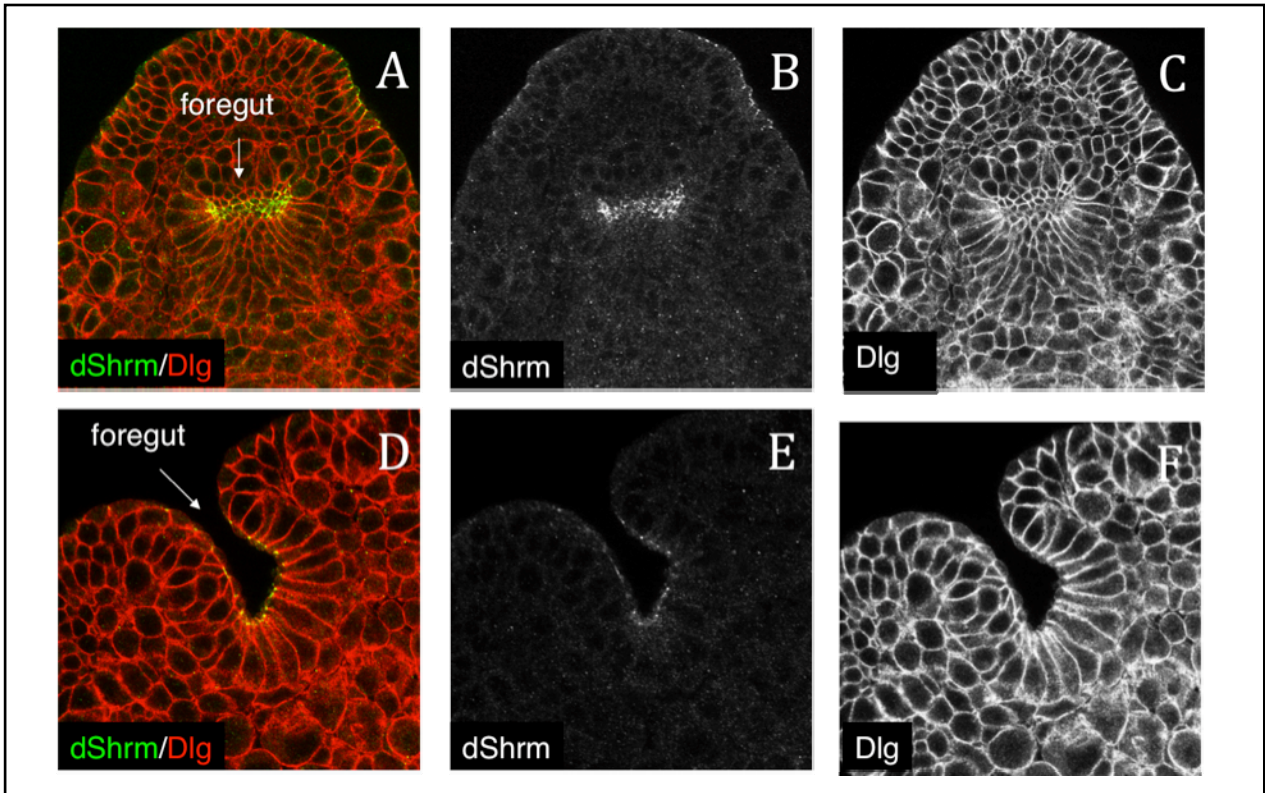


**Figure 9. dShrm protein is expressed in the invaginating foregut of the embryo. W1118 embryos at stage 10 stained to detect dShrmA (green) and Dlg (red), oriented with anterior at the top**

and that this protein appears to be localized to the apical surface of cells. This is consistent with experiments showing that dShrmB is specifically localized to the apical plasma membrane (see over expression data below).

*In situ* hybridization was performed to detect dShrm RNA. The staining is seen in Figure 10A; cellular blastoderm staining localizes roughly to the middle of the embryo, whereas in Fig. 10B, hybridization is detected in the tracheal system of a later-stage embryo. The results from *in situ* hybridization support those seen from immunofluorescence, where dShrm expression is

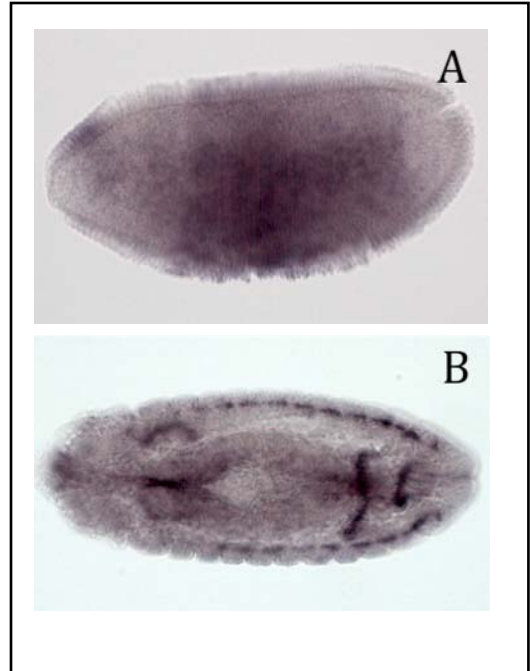


Figure 10. *in situ* hybridization of dShrm RNA in a cellular blastoderm (lateral view, A) and stage 14 embryo (dorsal view, B)

widespread in the ectoderm of early-stage embryos. However, once gastrulation has begun there is a detectable pattern of localization in populations of tubules and the ectoderm throughout the embryo.

### III B. Gain-of-function analysis of dShrmA and dShrmB

#### Transgenic *Drosophila* Lines

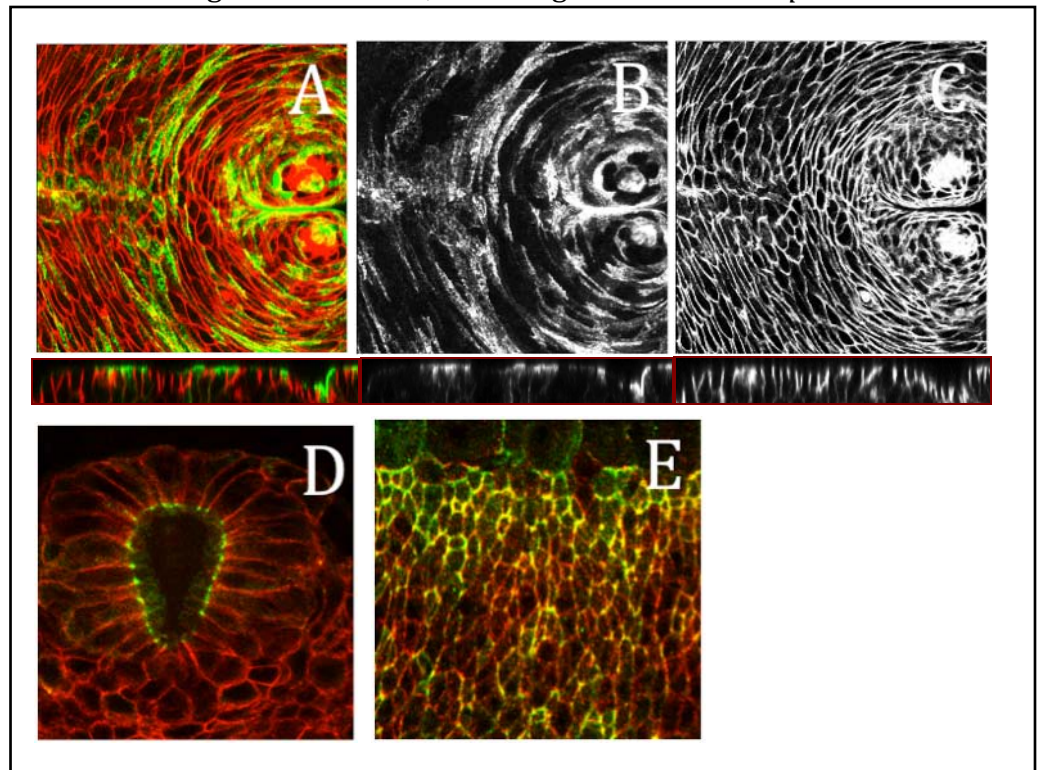
One of the strengths of *Drosophila* is the ability to achieve high level, tissue-specific over expression of proteins using the Gal4-UAS system. To utilize this system,

cDNAs encoding dShrmA, dShrmB, or DN-dRok were cloned into the P-element transposon vector pUAST that also contain the a  $w^+$  dominant marker, and the resultant plasmids were sent to Genetic Services Inc for production of UAS-dShrmA, UAS-dShrmB, and UAS-DN-dRok transgenic flies. Transgenic flies were characterized by two criteria. First, lines were assessed by western blot and immunofluorescent staining to verify expression of the protein of the correct size. Secondly, these lines that expressed proteins were mapped in order to identify the chromosomal insertion site and facilitate genetic analysis. For mapping, flies that are  $w^-$ ; Sp/Cyo; Dr/TM3 Sb (mapping stock) were used to track segregation of the transgenes. The mapping is accomplished by first crossing the transgenic flies to the mapping stock, and from that cross selecting  $w^+$  flies with either Sp or Cyo, and either Dr or TM3 Sb. These flies are then mated with  $w^{1118}$  flies, and based on the segregation of phenotypes in the offspring the transgene's chromosomal location can be determined.

There is currently no loss-of-function mutant for the dShrm gene, so gain-of-function experiments were used to determine if abnormal dShrm expression perturbs the cellular behavior and architecture. This method of analysis provides insight into the function of a protein, but has limitations. The major drawback to this approach is that over expression of proteins may not only disrupt the specific pathway and interactions in question, but may also cause unwanted changes in unrelated pathways. Due to this limitation, the results of gain-of-function experiments must be interpreted with that potential consequence in mind.

There are three goals to the gain-of-function analysis. They are: 1) to determine the subcellular localization of ectopically expressed dShrm proteins, 2) to determine the consequences of over-expression, and 3) to assess the interaction, if any, between dShrm and dRok. This allows for analysis of the cellular phenotypes to provide insight as to the function of dShrm. We predict that a dShrm-dRok interaction is vital to the control of aspects of cell morphology during embryogenesis. The Gal4-UAS expression system was utilized to direct over-expression of transgenes in assorted specific tissues [34]. The *engrailed* driver line was used to study over-expression in segmental stripes throughout the embryo, the posterior compartment of the wing discs of larvae, and wings of adults. The *pannier* driver

was used to determine the effects of over-expression in the dorsal third of the developing ectoderm, and the *GMR* driver was used for



over-expression in the tissues of the eye. The

Figure 11. Localization of ectopic dShrmA and dShrmB in the embryonic ectoderm. Dorsal view of a stage 15 *dShrmB;arm-Gal4* (A-C) embryo stained to detect dShrmB (green in A, and B) and Dlg (red in A, and C). Z-sections located below corresponding images. D, E show the gut (D) and leading edge (E) of a *dShrmA;arm-Gal4* embryo. In D, red is Dlg and green is dShrmA. In E, red is Arm and green is dShrmA.

*Armadillo* driver was used to direct ubiquitous over-expression. The effects of over-expression using these various drivers on dShrmA and dShrmB are summarized in Table 1.

We first wanted to verify the localization of the transgenic protein in comparison to endogenous dShrm proteins. dShrmA and dShrmB were expressed ubiquitously and the embryos were stained to detect dShrm. Figure 11A-C shows the ectoderm and posterior spiracles of a stage 15 embryo with UAS-dShrmB over-expressed using the *armadillo-Gal4* driver. Panels A (red) and C show Dlg staining, which distributes to the lateral membrane as seen in a Z-section through the ectoderm in lower panels. dShrmB, seen in panels A (green) and B, is mosaically expressed ectopically and localizes to the apical plasma membrane as is seen in A' (green) and B'. Over expression of UAS-dShrmA with the *arm* driver shows that ectopically expressed dShrmA is detectable apical to Dlg in the gut (Figure 11D), and colocalizes with Arm in the AJ (Figure 11E). This is interesting, as this localtion is spatially analogous to Shrm expression in vertebrates at the tight junctions. In their respective organisms here, these junctions are located at the most apical region of the lateral sides. This conservation of localization suggests that the positioning of Shrm proteins at the most apical junctions is required for the assembly of a circumfrential actomyosin network that can cause a constriction in the apical domain. These results show that dShrmA and dShrmB have distinct localization patterns, which suggests a difference in function and mechanism of action as well. These results also confirm our predictions for the endogenous distributions of these proteins, which predicts localization of dShrmA in the AJ of epithelial cells and localization of dShrmB to the apical surface of epithelia of tubules.

### III B.2 Phenotypes caused by dShrm over expression

The embryos in Fig. 12 show the morphological effects of over-expressing UAS-dShrmB under control of the *Arm-Gal4* driver. Fig. 12A and Fig. 12B (enlarged) show the mosaic expression of dShrm (green) in a stage 14 embryo, which causes holes in the ectoderm. Red staining is Dlg, showing the lateral edges of cells. These ectodermal abnormalities are manifested in the cuticles deposited

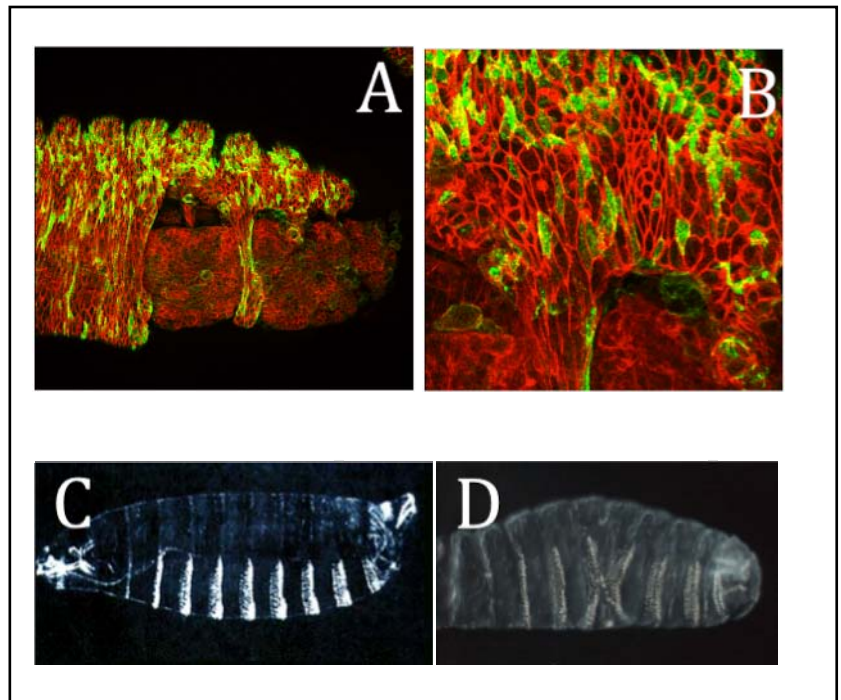
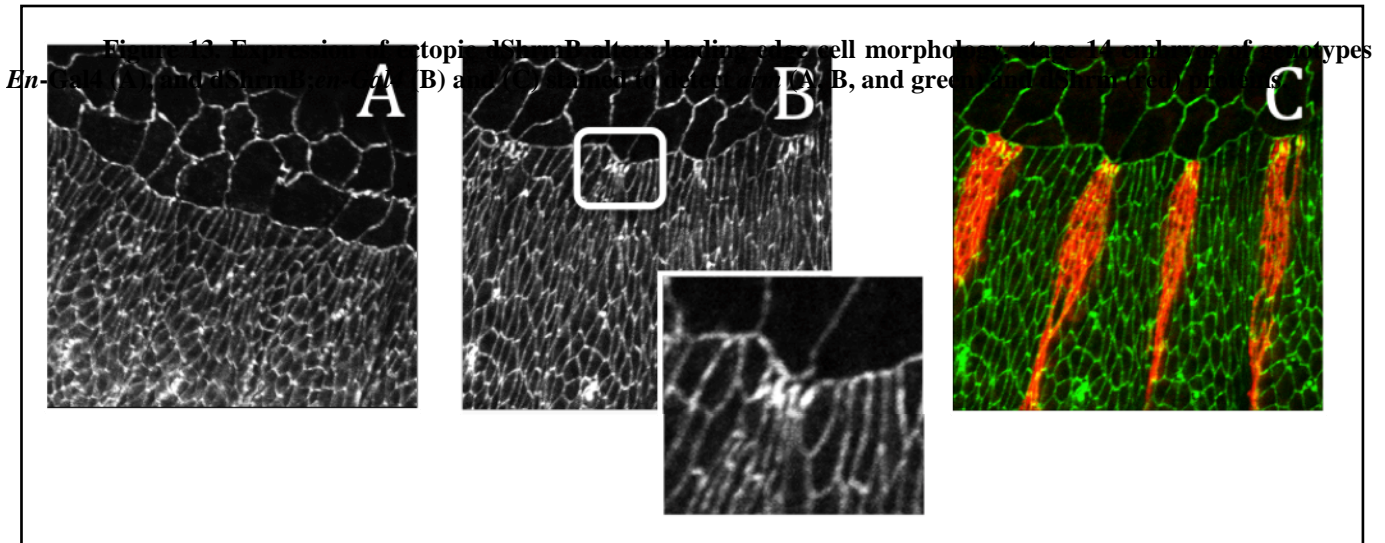


Figure 12. Phenotypes caused by ubiquitous dShrmB over expression. (A) and (B), dShrmB; *arm-Gal4* embryo, stage 14 stained with antibodies to dShrm (green) and Dlg (red). (C), control cuticle, and (D) *dShrmB; arm-Gal4* cuticle

by the embryos starting during stage 15. Fig. 12C shows a normal cuticle (<http://www.biologie.uni-erlangen.de/entwbio/klingler/gallery/larvae.html>) in comparison to Fig. 12D. Fig.12D shows a pinching of the cuticle where the space between the 6<sup>th</sup> and 7<sup>th</sup> denticular bands is absent. Since the cuticle is deposited by the ectoderm as the embryo is nearing the end of embryonic development, these abnormalities in the cuticle can be attributed to defects in the ectoderm caused by ectopic dShrmB over-expression.

The effects of ubiquitous dShrmB over expression causes disruption which limits the use of these embryos for assessing dShrmB gain of function. *UAS-dShrmB;pnr-*

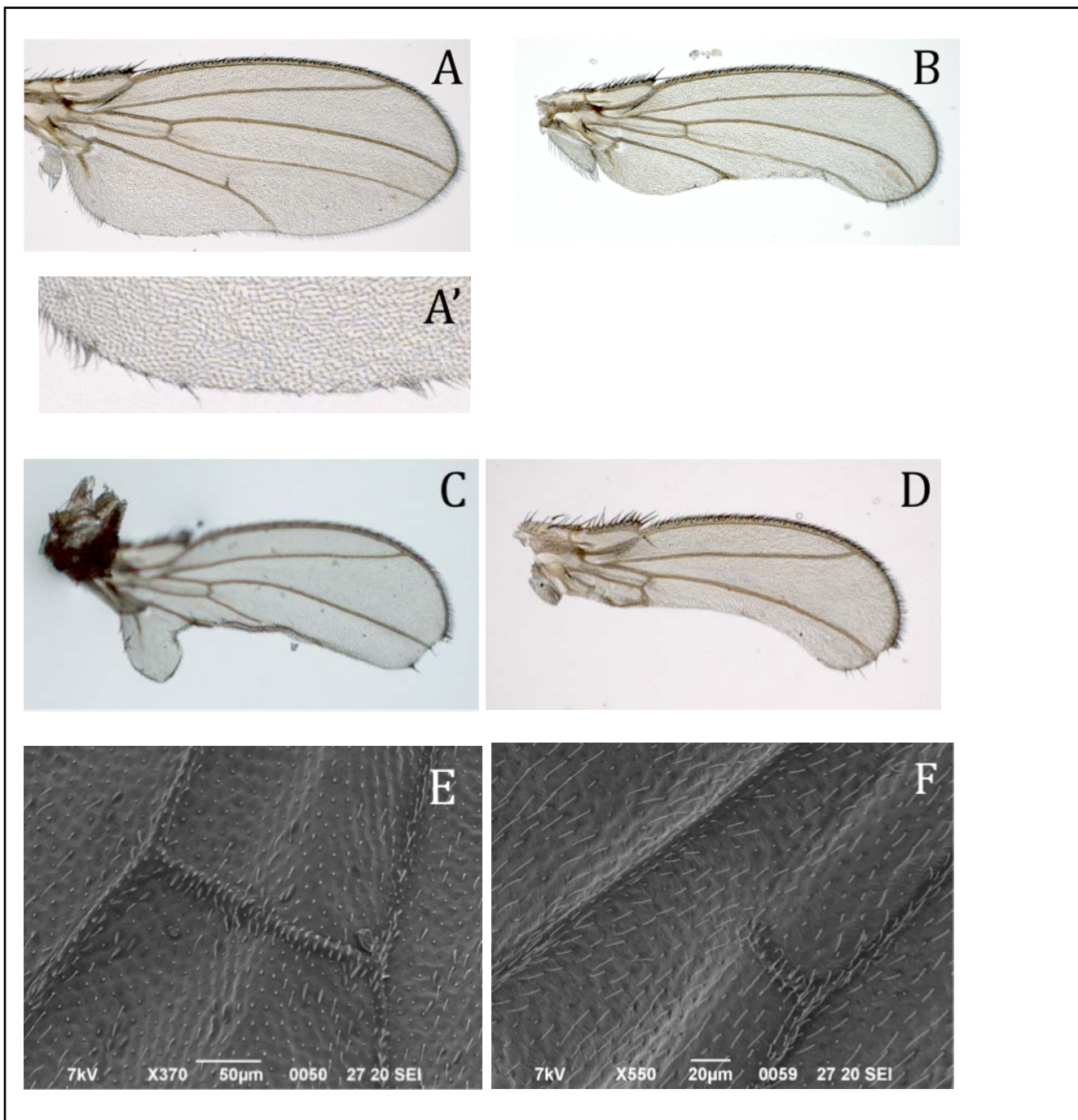
*Gal4* flies survive into adulthood, as the embryos have less damaging defects and a higher survival rate than with the *Arm-Gal4* driver. In these flies, the effects of incorrect dorsal closure are apparent. Minor thorax and abdomen defects are apparent, and most notably the scutellum is decreased in size, often misshapen, and has incorrect bristle number and directionality of the large bristles found on the scutellum (data not shown).



While the ubiquitous over-expression of dShrmB did create interesting phenotypes in the embryo, these often caused very severe defects or lethality. This damage to the embryo limits the practical uses of the *arm-Gal4* driver for studying the effects of dShrm over-expression.

Due to the mosaic nature of the *arm* driver and the variability in phenotype, we opted to further analyze dShrmB by ectopically expressing it in more specific regions of the embryo and imaginal discs. To do this, we first expressed dShrmB in the posterior portion of each segment and the posterior half of the wing imaginal disc using the *engrailed* driver. The embryos in Fig. 13 are stage 14, showing a region of the embryo where the leading edge of the ectoderm meets the amnioserosa during dorsal closure. The cells in the

amnioserosa of both control and *dShrmB;en-Gal4* embryos are larger than ectoderm cells and do not express the ectopic dShrmB in the *dShrmB;en-Gal4* embryos (B, C). (A) shows a control *En-Gal4* embryo with Arm protein staining. The leading edge cells are elongated as compared to the rest of the ectoderm. In (B), the *En-Gal4;UAS-dShrmB* embryo shows clusters of cells in the leading edge that are morphologically distinct (apically constricted) from the rest of the leading edge cells (also stained with Arm antibodies). One of these clusters is seen in the boxed region. In C, green staining is Arm and red is dShrmB, and the clusters of cells in the leading edge that are morphologically distinct from the rest are seen to correspond to those in the stripes of dShrmB over-expression. This shrinking of the surface of the cells is reminiscent of the activity of vertebrate Shrm family members *in vivo*.



Wings A-D in Fig 14 are all from *UAS-dShrmB;En-Gal4* flies, and show a range of defects that are seen with over-expression by the *engrailed* driver. In addition to causing ectopic expression of the transgene in stripes within the embryo, *En-Gal4* causes overexpression in the posterior compartment of the developing wing discs. Morphological changes in the wing disc are manifested as defects in the adult wings as is seen above. The range of defects with this over-expression is broad, from small defects in the wing

**Figure 14. Ectopic dShrmB expression disrupts wing morphogenesis. (A), (B), (C), (D), dissecting scope images of dShrmB;en-Gal4 wings, oriented posterior edge down. (E), SEM image of an En-Gal4 control wing at X370 (F), SEM image of a dShrmB;en-Gal4 wing at X550**

defects that are seen with over-expression by the *engrailed* driver. In addition to causing ectopic expression of the transgene in stripes within the embryo, *En-Gal4* causes overexpression in the posterior compartment of the developing wing discs. Morphological changes in the wing disc are manifested as defects in the adult wings as is seen above. The range of defects with this over-expression is broad, from small defects in the wing

crossveins (Fig. 14A) to loss of the entire posterior compartment (Fig. 14D). Figure 14B and C show loss of portions of the posterior wing as well as defects with the veins in the posterior of the wing. There is also a disruption and loss of bristles along the posterior edge of the wing, as seen in Fig. 14A'. It is important to note that the anterior compartment of these wings is not altered by the over-expression, as the driver does not direct expression of the transgene in that region. SEM data, seen in Fig. 14E (*En-Gal4* control) and Fig. 14F (*UAS-dShrmB;GMR-Gal4*), indicates that there are no planar cell polarity defects seen in these wings, as all the bristles are arranged normally and point in the correct direction (distally). The SEM data also verifies disruption of the crossvein.

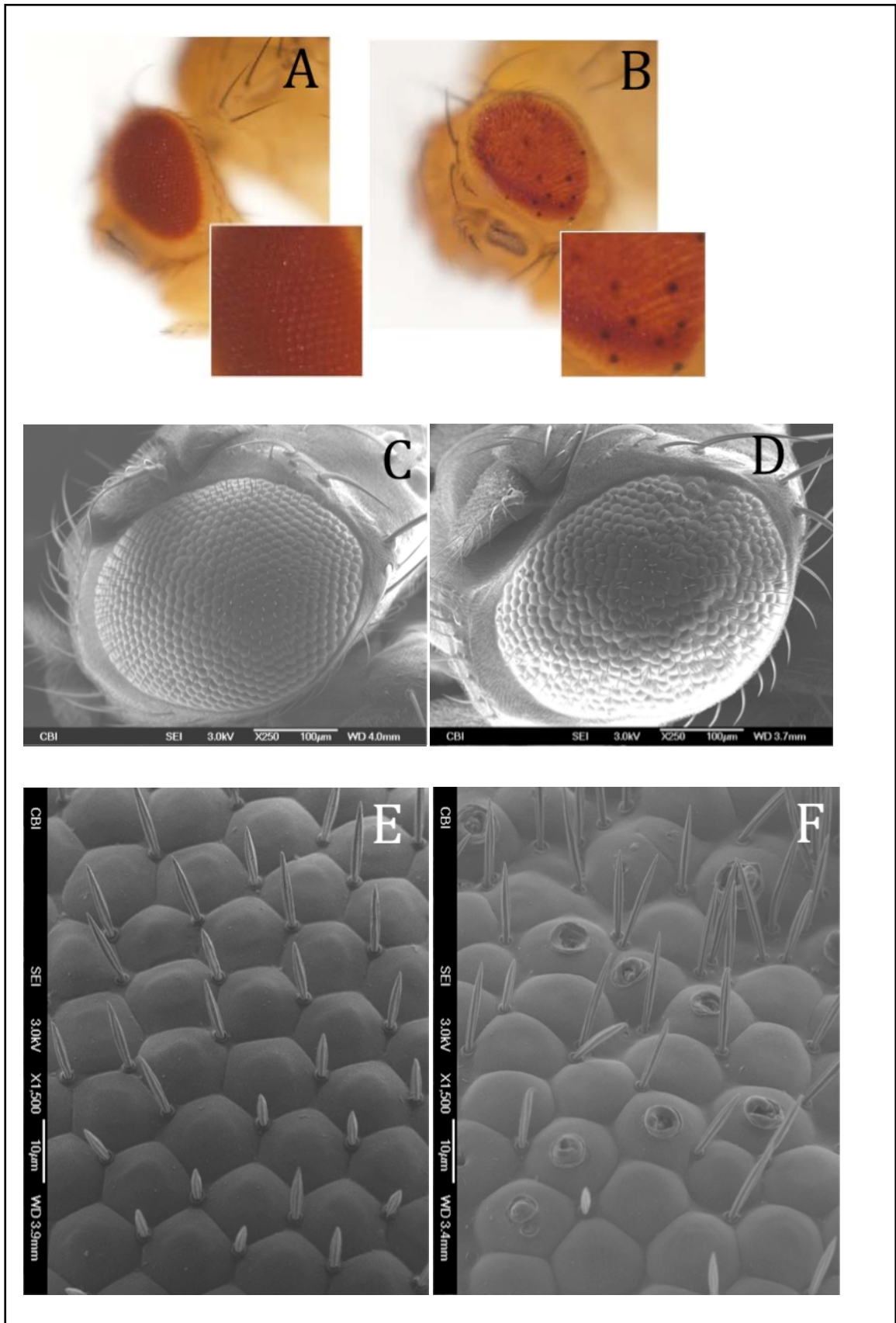


Figure 15. Ectopic dShrmB expression alters eye morphogenesis. (A), control *GMR-Gal4* fly as seen under the dissecting scope, (B), dShrmB-*GMR-Gal4* viewed with a dissecting scope. (C-F), SEM images of *GMR-Gal4* control (C, E) eyes and dShrmB;*GMR-Gal4* (D, F) eyes.

To determine if *Drosophila melanogaster* is a useful model system for studying the Shrm family of proteins, it must be shown that the results in flies can be translated to vertebrates. Since the vertebrate forms of Shrm are expressed in polarized epithelial tissues, it is of use to study dShrm in a variety of analogous tissue types. The eye discs and eyes provide this type of tissue (as do other discs and embryos), are very sensitive to perturbation, and may be studied into adulthood. For these reasons, UAS-dShrmB and UAS-dShrmA were over-expressed in the eye under control of the GMR-Gal4 driver. Data for *dShrmB;GMR-Gal4* over expression is seen in Figure 15. dShrmB causes a more robust phenotype when over expressed with the *GMR-Gal4* than does the dShrmA isoform. This is likely due to molecular interactions with the *GMR-Gal4* locus and dShrm insertion sites. Alternatively, the tissue in the developing eye may be more sensitive to excess dShrmB than dShrmA.

In Fig. 15A and B, dissecting scope images show the eyes of (A) a control GMR-Gal4 fly and (B) a *UAS-dShrmB;GMR-Gal4* fly. The insets in (A) and (B) show close-up ommatidia, some of which are black in the dShrmB mutant. In SEM views (C-F) it is apparent that the GMR-Gal4 line (C, E) has a minor rough eye phenotype, but shows overall regularity in ommatidial and bristle spacing and directionality. In the dShrmB over-expression flies (D, F), however, there is a loss of overall organization, incorrect bristle placement, and structurally deformed ommatidia, which correspond to the black spots seen under the dissecting scope. The defects seen with bristle placement are likely due to overall organizational defects as opposed to defects in bristle development, as the bristles arise from a separate population of cells than the rest of the eye. The black ommatidia are likely dead cells beneath the corneal surface, as this is a phenotype observed with apoptotic

cells in the eye [35]. Since the eye arises from an eye imaginal disc, analysis of *UAS-dShrmB;GMR-Gal4* imaginal discs from larvae would lend insight into the developmental and organizational abnormalities in these flies

### III B.3 Analysis of dShrmA gain-of-function phenotypes

To begin characterization of dShrmA function, we initially expressed it ubiquitously in the ectoderm using the *arm-Gal4* driver. While this resulted in robust expression, it

caused 100% lethality. The phenotype of a representative *UAS-dShrmA;Arm-gal4* embryo is shown in Fig. 16. These embryos display a severe phenotype in germ band retraction and dorsal closure. In order to determine the basis for the observed phenotypes, we analyzed the integrity of the ectoderm by staining embryos to detect E-cadherin, a core component of Adherens Junctions. In

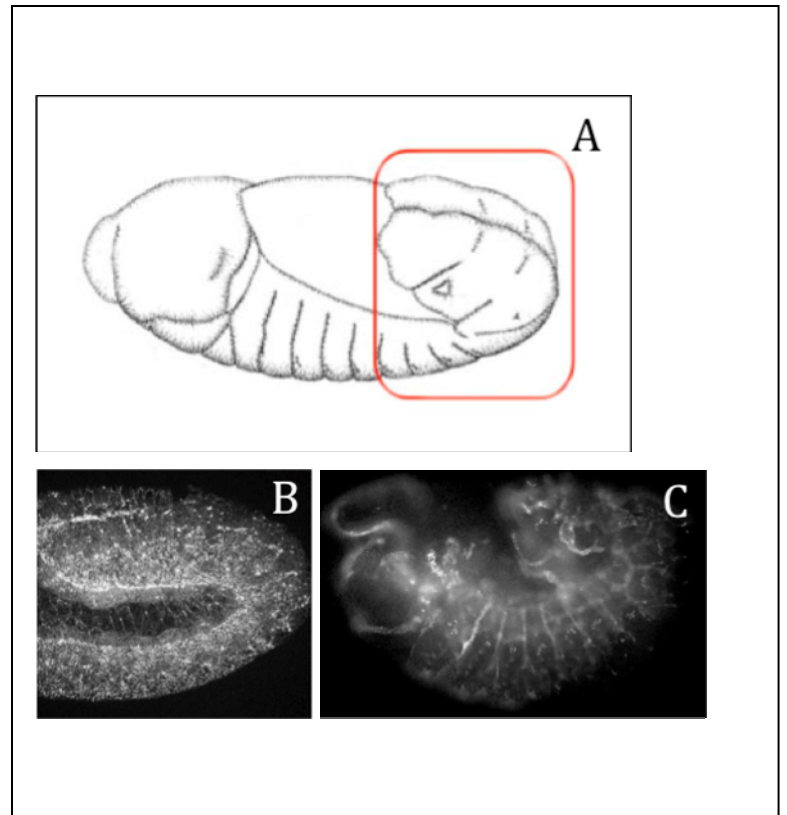


**Figure 16. Ectopic dShrmA expression causes AJ disruption. (A), cartoon with boxed region showing analogous region as in (B). (B,C), E-cadherin, Arm staining (respectively) in embryos during germ band retraction**

these embryos, E-cadherin is still expressed in many cells and exhibits the

correct subcellular distribution. However, we also observed large patches of the ectoderm in which E-cadherin staining appears to be lost (Fig. 16B), suggesting that the AJs are

disrupted by dShrmA over-expression. Structural defects in *UAS-dShrmA;Arm-gal4* embryos are seen with the Arm staining in the ectoderm of a stage 12 embryo undergoing germ band retraction (Fig. 16, boxed area in cartoon in panel A shows analogous region for location in panel B).

### ***Pnr-Gal4* over-expression of dShrmA**

While our initial analysis of dShrmA function proved informative, the dramatic defects in embryonic development made it difficult to assess the actual activity of dShrmA at the cellular level. To circumvent

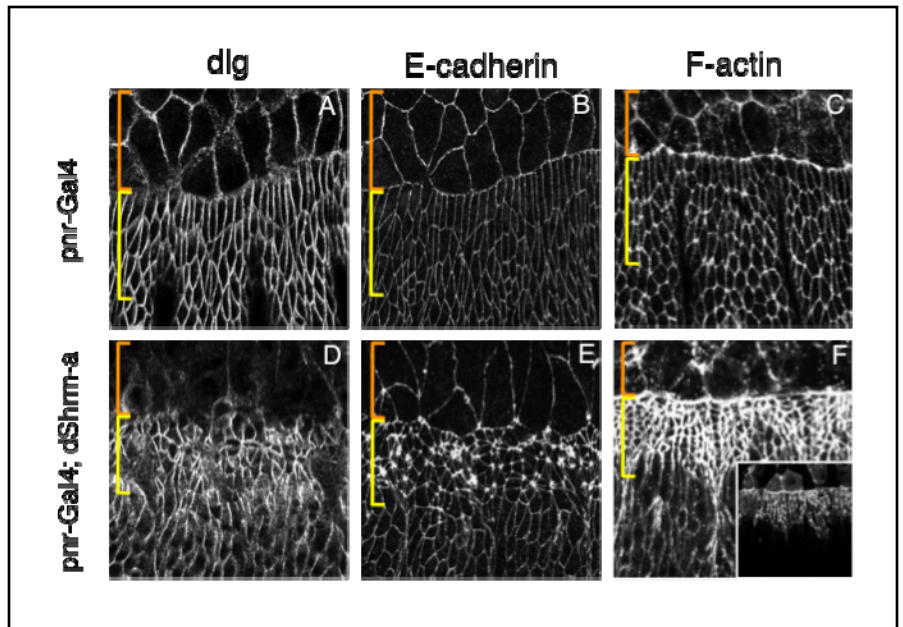


**Figure 17. Ectopic dShrmA expression causes apical constriction. (A-C), *pnr-Gal4* embryos during dorsal closure, stained to detect *dlg*, E-cadherin, and F-actin, respectively. (D-F), *dShrmA;pnr-Gal4* embryos during dorsal closure, stained to detect *dlg*, E-cadherin, and F-actin, respectively. (F inset), dShrmA staining. Orange brackets denote amnioserosa, yellow brackets denote the *pnr* expression domain.**

the global defects in embryogenesis caused by ubiquitous dShrm over expression, we elected to express dShrmA in a more restricted manner using the *pnr-Gal4* driver. This line drives expression in the dorsal third of the ectoderm, including the amnioserosa and the leading edge. Expression of dShrmA by the *pnr-Gal4* driver also results in near complete embryonic lethality, but this is due to defects in dorsal closure attributed to disruption of leading edge cell morphology (Figure 17). To begin to analyze this phenotype, *UAS-dShrmA;Pnr-gal4* embryos were collected and assayed by

immunofluorescence staining and confocal microscopy in order to assess cell morphology, cell-cell adhesion, and cytoskeletal organization. In Figure 17, control cell morphology and protein localization is seen in the control *pnr-Gal4* embryos. In the control embryos, the ectoderm cells in the *pnr-Gal4* expression domain are elongated along the dorsal-ventral axis, are all approximately the same size and shape, and are arranged in rows along the dorsal-ventral axis (Fig. 17 A-C, yellow bracket). In contrast, in the *pnr-Gal4; dShrmA* embryos, the cells within the *pnr-gal4* expression domain have irregular lateral edges in (D) as compared to (A). Embryos stained to detect E-cadherin show that while the AJs are largely intact, there are regions where E-cadherin is highly enriched and appears to be clustered at the cell membrane. It is unclear at this time if this represents cells that are highly constricted or if these are tri-cellular junctions and represent regions of high contractile activity. Consistent with the notion that these cells are undergoing apical constriction, there is a dramatic increase in actin signal in the constricted cells in the leading edge (Figure 17F). This increase in actin signal could be attributed to either an increase in actin in this area, or an increase in the signal as a result of apical constriction and decreased area with the same amount of actin more condensed and therefore appearing brighter. Taken together, these data are indicative of apical constriction and suggest dShrmA has the ability to activate the contractile apparatus in these cells to change cell morphology. This is supported by additional observations from the lab that show that activated myosin II is enriched in the adherens junctions, and tri-cellular junctions in particular, in cells that expresses dShrmA (work from the Hildebrand lab, in press).

To follow up on the above results, cell morphology was also assayed using scanning electron microscopy (SEM, Fig. 18). Using this approach, we see that the leading edge cells in control cells are flat and elongated. In contrast, the cells at the leading edge of the *dShrmA;pnr-Gal4* appear to have rounded apical surfaces, are smaller in size, and are

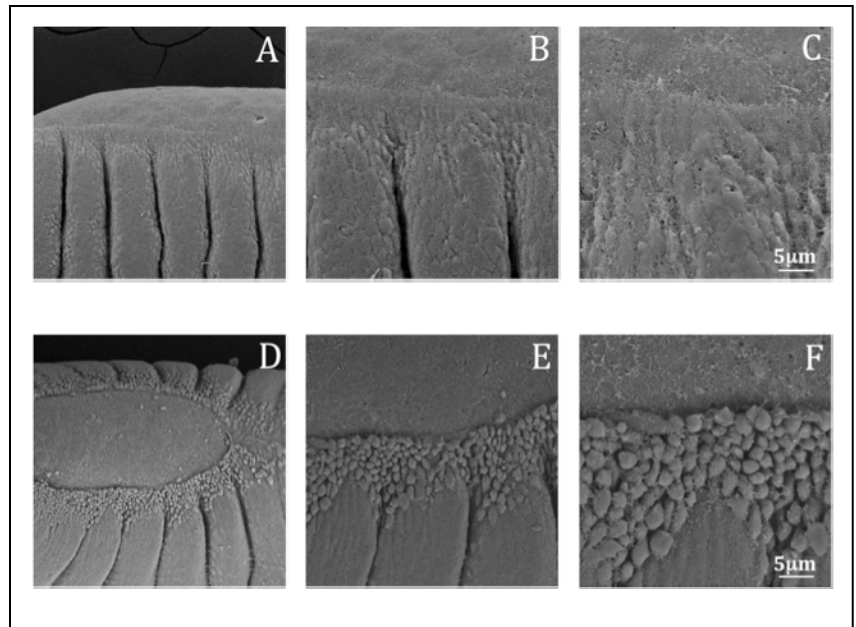


**Figure 18. Ectopic dShrmA causes abnormal cellular morphology. (A-C), SEM images of a *pnr-Gal4* control embryo, (D-F), SEM images of a *dShrmA;pnr-Gal4* embryo. Both embryos are stage 14, oriented with dorsal up**

disorganized (Fig 18C). This phenotype appears to be the result of apical constriction that creates causes the apical plasma membrane of these cells to bulge outward. This could result from apical constriction occurring at the adherens junctions due to a circumferential contractile network and a failure of these cells to internalize apical membrane to compensate for the decrease in apical size. This effect of apical constriction in the cells at the leading edge is similar to the constriction seen by over expression of dShrmB in this domain (Figure13).

The above analysis of tissue behavior, cell morphology, and cytoskeletal organization strongly suggests that dShrmA can induce robust apical constriction in

ectodermal cells of the *Drosophila* embryo. These results also suggest that the activity of Shrm proteins is conserved in invertebrates.

### III B.4 The role of dRok in dShrm activity

In vertebrates, the activity of Shrm3 in apical constriction is dependent on the ability to bind Rho kinase and recruit it to the tight junctions [6, 31]. We hypothesized that dShrmA is functioning in an analogous manner, since it contains an SD2 motif and causes robust apical constriction *in vivo*. To test this hypothesis, we expressed a version of

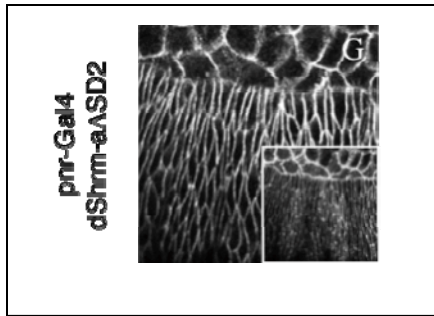


**Figure 19. An interaction between dShrm and dRok mediates apical constriction. Stage 12 embryo ectopically expressing dShrmA lacking the SD2 domain (inset shows dShrm expression), stained to detect Arm**

dShrmA that lacks the Rok binding SD2 motif (dShrm- $\Delta$ SD2) using *pnr-Gal4* driver. This protein is expressed at high levels and exhibits the correct distribution, but does not cause any overt phenotype of apical constriction (Fig 19). This indicates that the SD2 domain is necessary for the function of the dShrmA protein to effect physical changes in cell shape.

To verify the role of Rho-kinase in constriction, we co-expressed dShrmA and the region of *Drosophila* Rho-kinase (dRok) that binds to the dShrm SD2 motif. This domain is termed the SBD, for Shroom Binding Domain, and spans amino acids 724-938. Expression of the SBD protein alone does not cause any overt phenotype in dorsal closure or the leading edge (not shown). Over expression of dShrm and a DN-dRok together would theoretically inhibit the effects seen by over expression of dShrmA by itself. When this dRok-SBD is co-expressed with dShrmA, it is recruited to the AJ and codistributes with

dShrmA (Figure 20). Importantly, this protein appears to function as a dominant-negative and reverts the constriction phenotype that is seen when dShrmA is over-expressed alone (Figure 20). This data suggests that dShrm proteins function via dRok to control actomyosin contractility and regulate cell morphology.

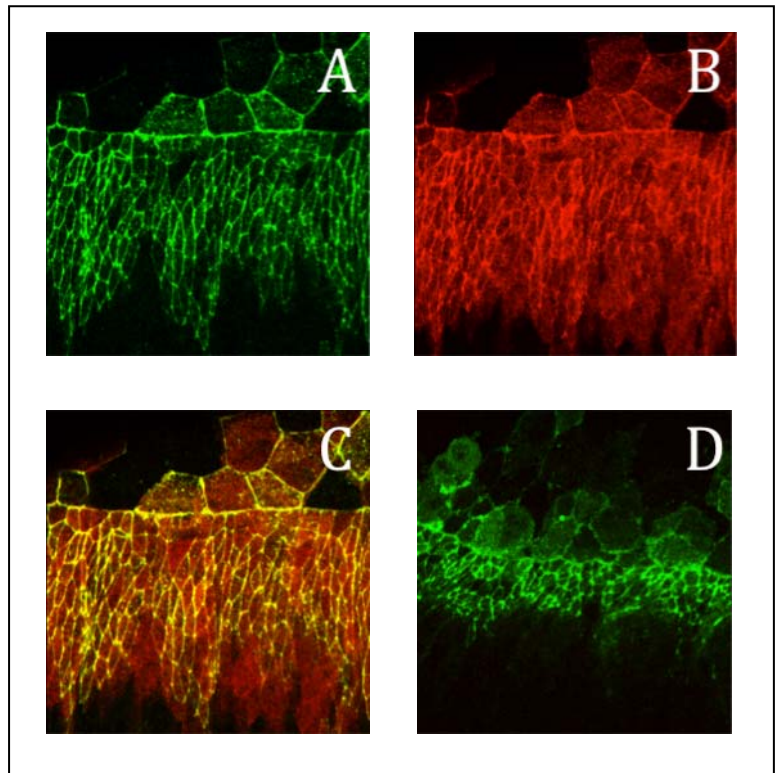


**Figure 20.** Co-expression of a functionally DN-dRok and dShrm inhibits the effects of ectopic dShrm expression by itself. Stage 12 embryos of the phenotype *dShrmA;dRok-SBD;pnr-Gal4* (A-C) and *dShrmA;pnr-Gal4* (D), images are of the leading edge with dorsal oriented up. Embryos are stained to detect dShrmA (green in A, C, D) and Rok-SBD (red in B, C).

#### IV. DISCUSSION

This project describes the initial *in vivo* characterization of the *Drosophila* ortholog of vertebrate Shroom proteins. In this work we have shown that the *dShroom* locus encodes at least two protein isoforms, and these proteins appear to mediate different functions. We also show that dShrm proteins likely function in polarized populations of epithelial cells to control actomyosin contractility, and thus control cell morphology during embryogenesis.

Table 1 summarizes localization and expression data that has been compiled during these studies.

**Table 1. Localization and expression effects of Shrm family members (lethality due to apical constriction)**

Shrm family member	Endogenous localization	Constriction in MDCK cells	Constriction in <i>Drosophila</i> embryos	Ubiquitous over expression lethality	<i>Pnr-Gal4</i> driven lethality	<i>En-Gal4</i> driven lethality	<i>GMR-Gal4</i> driven lethality
Shrm3	Tight Junctions	+++	---	---	(not determined)	(not determined)	(not determined)
dShrmA	Adherens Junctions	---	---	+++	+++	+++	+
dShrmB	Apical Plasma Membrane	+	+	+	+	---	+++

Using unique sets of reagents that we developed, we have shown that dShrmA and dShrmB exhibit unique subcellular localization, with dShrmA targeted to the adherens junctions, and dShrmB targeted to the apical plasma membrane. It also appears from our

analysis that dShrmA and dShrmB are expressed in different populations of epithelial cells. For example, dShrmA appears to be widely expressed in ectodermal epithelia and epithelial cells of some imaginal discs, and the follicle cells of the ovary. In contrast, dShrmB appears to be expressed in polarized epithelia that compose tubes in the tracheal system. Our data presented here also suggests that dShrmA and dShrmB may function differently in various cell types. This is most clearly seen when these two proteins are ubiquitously over expressed in the embryo. Ubiquitous over expression of dShrmA results in complete lethality and severe defects in the ectoderm that block several developmental processes. In contrast, ubiquitous dShrmB over expression results in significantly milder phenotypes and does not cause significant apical constriction. This is also seen when dShrmA and dShrmB are expressed using the *pnr*-Gal4 driver, as dShrmB does not induce the severe defects observed following dShrmA expression with the same driver.

Another very interesting observation is the differential localization of dShrmA and dShrmB. It has been shown by others in the lab that dShrmA contains a direct actin binding domain, which appears to be essential for its localization to the AJ. In contrast, the localization of dShrmB appears to be independent of the actin cytoskeleton. The localization of dShrmA to the AJ is also interesting when compared to the localization of vertebrate Shrm3. This distribution of dShrmA is analogous to that of Shrm3, however Shrm3 is localized to the tight junctions. This suggests that dShrmA and Shrm3 have retained the same distribution during animal evolution, but most likely utilize somewhat different mechanisms to localize, although both utilize the actin cytoskeleton. Also, it should be pointed out that dShrmA and Shrm3 are both capable of inducing apical contractile networks only when they are localized to this apicolateral position in the cell,

suggesting that this region of the cell is favorable or permissive for assembling contractile networks.

## V. FUTURE EXPERIMENTS

Our studies have shown that dShrmB has pronounced effects on imaginal disc development, and causes dramatic defects in these tissues when over expressed. We would like to do more detailed analysis of these phenotypes at the cellular level to understand the basis for these phenotypes. I am particularly interested in studying the cellular morphology following dShrmB over expression in the eye and if there are alterations in cell shape, adhesion, or cytoskeleton organization. In addition, it would be useful to verify that the dShrmB phenotypes are not caused by changes in cell proliferation or survival as opposed to changes in cell morphology.

Currently all the analysis of dShrm activity has come through the use of gain-of-function analysis. While this is useful, there are drawbacks to this approach. Most obvious is that it does not indicate what the endogenous role of a given protein is during a given biological process. Therefore, one of the major deficiencies in these studies is the lack of loss-of-function analysis. These are crucial in order to show if dShrm activity is necessary for any developmental processes or morphogenic events. These studies require the production of mutants by either P-element excision or by the use of RNAi lines. RNAi lines are now available and will be used to knock down dShrm function during embryogenesis. This will allow us to then further assess the function of dShrm.

## VI. MATERIALS AND METHODS

Transgenic lines carrying UAS-dShrmA, UAS-dShrmB, UAS-dShrmA  $\Delta$ SD2, and UAS-dRok-SBD (containing the Shrm Binding Domain (SBD) of dRok) were generated by Genetic Services Inc. Driver lines of *pnr-GAL4*, *arm-GAL4*, *en-GAL4*, and *GMR-GAL4* were obtained from Dr. Beth Stronach (University of Pittsburgh), although they originated from the Bloomington Stock Center (Department of Biology, Indiana University). *w-; sp/cyo; dr/tm3sb* balancing line was obtained from Dr. Beth Stronach (University of Pittsburgh). All crosses were set up at 25°, and all embryos were collected from plates also at 25°C.

Cells or embryos were lysed in RIPA buffer, and proteins resolved by SDS-PAGE. Proteins were then transferred to nitrocellulose and probed with antibodies overnight at 4°C. Primary antibodies from this incubation were detected with HRP-conjugated secondary antibodies (1:2500, GE Health Systems), and detected using ECL.

Embryos were collected at 4-12 hours post fertilization, and dechorionated in 50% bleach for 3 minutes. They were then rinsed with water, collected in heptane, and fixed in a 1:1 mixture of 37% formaldehyde and heptane for 5 minutes with shaking at room temperature. Fixed embryos were devitellinized by vigorous shaking in a 1:1 heptane and methanol mixture, and dehydrated by rinsing three times in methanol. Embryos were rehydrated in PBS + 0.1% Triton (PBT) for 30 minutes, blocked 30 minutes in PBT + 4%

normal goat serum (NGS), and incubated overnight in primary antibody at 4°C. Primary antibodies were washed off in PBT 6 X 10 minutes, and embryos were blocked again in PBT + 4% NGS for 30 minutes. Embryos were then incubated in secondary antibodies for 2 hrs at room temperature in the dark, washed 6 X 10 minutes in PBT, and mounted on microscope slides in Vectashield (Vector Labs). Embryos that were stained with phalloidin were dechorionated and fixed as described, hand devitellinized, and stained as described.

Embryos were stained to detect dShrm, Arm, dE-cadherin, or membrane GFP, and analyzed by confocal microscopy with imaging parameters maintained constant across all samples. Images were acquired using a Biorad Radiance 2000 Laser Scanning System and a Nikon E800 microscope with 40X and 60X oil objectives, and processed using ImageJ or Photoshop.

For detection of dShrm proteins, antisera was produced in rats using bacterially expressed proteins of amino acids 1-183 for dShrmA (R20, R21, and R22) and 1144-1576 for dShrmA/B/C (R11 and R12), using protein segments from the dShrmA isoform. Antibodies were affinity purified from the antisera, and all produced similar results. Other antibodies used are: anti-Disc Large (Dlg) mAb 4F3 (1:400 DSHB), anti-Armadillo (Arm) mAb N2 7A1 (1:100, DSHB), anti-Fasciclin III (Fas) mAb 7G10 (1:400, DSHB); anti-Myc mAb 9E10, (1:100, a gift from Dr. Ora Wiesz, University of Pittsburgh); anti-E-cadherin mAb (1:400, BD Bioscience); anti-phosphotyrosine mAb 4G10, (1:1000, Upstate), TRITC-phalloidin (Sigma), To-Pro 3 (Invitrogen), goat anti-mouse, goat anti-rat, or goat anti-rabbit secondary antibodies conjugated to Alexa-488, Alexa-568, or Alexa-633 (1:400, Invitrogen).

Embryos were collected and fixed as with immunofluorescence for in situ hybridization, and then incubated in MeOH at -20°C for a minimum of 24 hours. They were then rinsed in fresh MeOH, and then in a 1:1 mixture of MeOH and PBT with 5% formaldehyde. The embryos were fixed in PBT-formaldehyde for 20 minutes with rocking, and rinsed in PBT. They were then incubated with proteinase-K for 3 minutes, rinsed in PBT 3X, and post-fixed in PBT-formaldehyde for 20 minutes. The embryos were rinsed 3X in PBT, and placed at 65°C for 1 hour in a 1:1 mixture of PBT and Hyb solution. They were then incubated overnight at 55°C in Hyb solution with probe, and rocked when possible. The probe is then removed and replaced with wash solution, and embryos rinsed in wash solution immediately, and incubated for 20 minutes at 55°C. The embryos were then incubated in a 1:1 mixture of wash solution and PBT at 55°C for 20 minutes, then rinsed 5X with hot (55°C) wash solution. They were cooled to room temperature, and incubated in anti-Dig AP antibody overnight at 4°C. After overnight incubation, the embryos were rinsed 3X quickly in PBT, and the 3X 20 minutes on the nutator. They were then rinsed in AP buffer, which was replaced with AP staining solution, and the embryos were transferred to a 9-well Pyrex dish in the dark during staining. The staining was allowed to occur for over 2 hours, checking periodically to determine development of staining. To stop the staining at the desired intensity, the embryos were washed in PBT 3X. For mounting, the embryos were transferred back to an Eppendorf tube, rinsed 3X quickly, and 3X 20 minutes in 100% EtOH, and transferred to a microscope slide. The EtOH was allowed to evaporate mostly but not completely, and Vectashield (Vector Labs) was used for mounting with a cover slip.

For SEM, embryos were collected as above and fixed as described by [36]. Fixed embryos were dehydrated through a graded series of EtOH, and washed through a graded

series of EtOH:hexamethyldisilazane (HMDS) to a final 100% HMDS. Embryos were then air dried, sputter coated, and imaged with a Jeol JSM6390LV SEM. Wings imaged by SEM were not fixed or dehydrated prior to sputter coating.

Cuticle preps were performed by collecting embryos from apple juice agar plates, and dechorionating in 50% bleach for 3 minutes before rinsing and transferring them to PBT. The PBT was then replaced by a 1:1 mixture of acetic acid and glycerol at 60°C for 30 minutes; the embryos were then placed a room temperature for at least 24 hours. The next day, the embryos were transferred to a 1:1 mixture of CMCP-10 and lactic acid and placed at 50°C overnight. They were then transferred to a microscope slide and mounted with Vectashield (Vector Labs).

## BIBLIOGRAPHY

1. Lecuit, T. and P.F. Lenne, *Cell surface mechanics and the control of cell shape, tissue patterns and morphogenesis*. Nat Rev Mol Cell Biol, 2007. **8**(8): p. 633-44.
2. Pilot, F. and T. Lecuit, *Compartmentalized morphogenesis in epithelia: from cell to tissue shape*. Dev Dyn, 2005. **232**(3): p. 685-94.
3. Apodaca, G., *Endocytic traffic in polarized epithelial cells: role of the actin and microtubule cytoskeleton*. Traffic, 2001. **2**(3): p. 149-159.
4. Sawyer, J.M., et al., *Apical constriction: a cell shape change that can drive morphogenesis*. Dev Biol, 2010. **341**(1): p. 5-19.
5. Lee, C., H.M. Scherr, and J.B. Wallingford, *Shroom family proteins regulate gamma-tubulin distribution and microtubule architecture during epithelial cell shape change*. Development, 2007. **134**(7): p. 1431-41.
6. Hildebrand, J.D., *Shroom regulates epithelial cell shape via the apical positioning of an actomyosin network*. J Cell Sci, 2005. **118**(Pt 22): p. 5191-203.
7. Plageman, T.F., Jr., et al., *Pax6-dependent Shroom3 expression regulates apical constriction during lens placode invagination*. Development, 2010. **137**(3): p. 405-15.
8. Bertet, C., M. Rauzi, and T. Lecuit, *Repression of Wasp by JAK/STAT signalling inhibits medial actomyosin network assembly and apical cell constriction in intercalating epithelial cells*. Development, 2009. **136**(24): p. 4199-212.
9. Bertet, C., L. Sulak, and T. Lecuit, *Myosin-dependent junction remodelling controls planar cell intercalation and axis elongation*. Nature, 2004. **429**(6992): p. 667-71.
10. Sawyer, J.K., et al., *The Drosophila afadin homologue Canoe regulates linkage of the actin cytoskeleton to adherens junctions during apical constriction*. J Cell Biol, 2009. **186**(1): p. 57-73.
11. Martin, A.C., M. Kaschube, and E.F. Wieschaus, *Pulsed contractions of an actin-myosin network drive apical constriction*. Nature, 2009. **457**(7228): p. 495-9.

12. Martin, A.C., et al., *Integration of contractile forces during tissue invagination*. J Cell Biol, 2010. **188**(5): p. 735-49.
13. Zhou, J., H.Y. Kim, and L.A. Davidson, *Actomyosin stiffens the vertebrate embryo during crucial stages of elongation and neural tube closure*. Development, 2009. **136**(4): p. 677-88.
14. Costa, M., E.T. Wilson, and E. Wieschaus, *A putative cell signal encoded by the folded gastrulation gene coordinates cell shape changes during Drosophila gastrulation*. Cell, 1994. **76**(6): p. 1075-89.
15. Zimmerman, S.G., et al., *Apical constriction and invagination downstream of the canonical Wnt signaling pathway require Rho1 and Myosin II*. Dev Biol, 2010. **340**(1): p. 54-66.
16. Corrigall, D., et al., *Hedgehog signaling is a principal inducer of Myosin-II-driven cell ingression in Drosophila epithelia*. Dev Cell, 2007. **13**(5): p. 730-42.
17. Widmann, T.J. and C. Dahmann, *Dpp signaling promotes the cuboidal-to-columnar shape transition of Drosophila wing disc epithelia by regulating Rho1*. J Cell Sci, 2009. **122**(Pt 9): p. 1362-73.
18. Nikolaidou, K.K. and K. Barrett, *A Rho GTPase signaling pathway is used reiteratively in epithelial folding and potentially selects the outcome of Rho activation*. Curr Biol, 2004. **14**(20): p. 1822-6.
19. Simoes, S., et al., *Compartmentalisation of Rho regulators directs cell invagination during tissue morphogenesis*. Development, 2006. **133**(21): p. 4257-67.
20. Riento, K. and A.J. Ridley, *Rocks: multifunctional kinases in cell behaviour*. Nat Rev Mol Cell Biol, 2003. **4**(6): p. 446-56.
21. Amano, M., et al., *Phosphorylation and activation of myosin by Rho-associated kinase (Rho-kinase)*. J Biol Chem, 1996. **271**(34): p. 20246-9.
22. Kawano, Y., et al., *Phosphorylation of myosin-binding subunit (MBS) of myosin phosphatase by Rho-kinase in vivo*. J Cell Biol, 1999. **147**(5): p. 1023-38.
23. Matsui, T., et al., *Rho-associated kinase, a novel serine/threonine kinase, as a putative target for small GTP binding protein Rho*. EMBO J, 1996. **15**(9): p. 2208-16.
24. Verdier, V., C. Guang Chao, and J. Settleman, *Rho-kinase regulates tissue morphogenesis via non-muscle myosin and LIM-kinase during Drosophila development*. BMC Dev Biol, 2006. **6**: p. 38.

25. Hildebrand, J.D. and P. Soriano, *Shroom*, a PDZ domain-containing actin-binding protein, is required for neural tube morphogenesis in mice. *Cell*, 1999. **99**(9): p. 486-497.
26. Dietz, M.L., et al., *Differential actin-dependent localization modulates the evolutionarily conserved activity of Shroom family proteins*. *J Biol Chem*, 2006. **281**(29): p. 20542-54.
27. Fairbank, P.D., et al., *Shroom2 (APXL) regulates melanosome biogenesis and localization in the retinal pigment epithelium*. *Development*, 2006. **133**(20): p. 4109-18.
28. Haigo, S.L., et al., *Shroom induces apical constriction and is required for hinge point formation during neural tube closure*. *Curr Biol*, 2003. **13**(24): p. 2125-37.
29. Taylor, J., et al., *The scaffold protein POSH regulates axon outgrowth*. *Mol Biol Cell*, 2008. **19**(12): p. 5181-92.
30. Hagens, O., et al., *A new standard nomenclature for proteins related to Apx and Shroom*. *BMC Cell Biol*, 2006. **7**: p. 18.
31. Nishimura, T. and M. Takeichi, *Shroom3-mediated recruitment of Rho kinases to the apical cell junctions regulates epithelial and neuroepithelial planar remodeling*. *Development*, 2008. **135**(8): p. 1493-502.
32. Amano, M., et al., *The COOH terminus of Rho-kinase negatively regulates rho-kinase activity*. *J Biol Chem*, 1999. **274**(45): p. 32418-24.
33. Chung, M.I., et al., *Direct activation of Shroom3 transcription by Pitx proteins drives epithelial morphogenesis in the developing gut*. *Development*, 2010. **137**(8): p. 1339-49.
34. Brand, A.H. and N. Perrimon, *Targeted gene expression as a means of altering cell fates and generating dominant phenotypes*. *Development*, 1993. **118**(2): p. 401-15.
35. Lee, H.G., et al., *The cell adhesion molecule Roughest depends on beta(Heavy)-spectrin during eye morphogenesis in Drosophila*. *J Cell Sci*, 2010. **123**(Pt 2): p. 277-85.
36. Mulinari, S., M.P. Barmchi, and U. Hacker, *DRhoGEF2 and diaphanous regulate contractile force during segmental groove morphogenesis in the Drosophila embryo*. *Mol Biol Cell*, 2008. **19**(5): p. 1883-92.